

Intralayer structure reconstruction of general weighted output-coupling multilayer complex networks

Xinwei Wang(王欣伟), Yayong Wu(吴亚勇), Ying Zheng(郑颖), and Guo-Ping Jiang(蒋国平)
Citation: Chin. Phys. B, 2026, 35 (**2**): 020202. DOI: 10.1088/1674-1056/adf180
http://cpb.iphy.ac.cn; http://iopscience.iop.org/cpb

What follows is a list of articles you may be interested in

An ADP-based robust control scheme for nonaffine nonlinear systems with uncertainties and input constraints

Shijie Luo(罗世杰), Kun Zhang(张坤), and Wenchao Xue(薛文超)
Chin. Phys. B, 2025, 34 (**6**): 060202. DOI: 10.1088/1674-1056/adbee1

Self-similarity of multilayer networks

Bing Wang(王冰), Huizhi Yu(于蕙芷), and Daijun Wei(魏代俊)
Chin. Phys. B, 2025, 34 (**1**): 010202. DOI: 10.1088/1674-1056/ad8a47

Bipartite consensus problems of Lurie multi-agent systems over signed graphs: A contraction approach

Xiaojiao Zhang(张晓娇) and Xiang Wu(吴祥)
Chin. Phys. B, 2024, 33 (**7**): 070204. DOI: 10.1088/1674-1056/ad3dca

Event-based nonfragile state estimation for memristive recurrent neural networks with stochastic cyber-attacks and sensor saturations

Xiao-Guang Shao(邵晓光), Jie Zhang(张捷), and Yan-Juan Lu(鲁延娟)
Chin. Phys. B, 2024, 33 (**7**): 070203. DOI: 10.1088/1674-1056/ad3dcb

Target layer state estimation in multi-layer complex dynamical networks considering nonlinear node dynamics

Yayong Wu(吴亚勇), Xinwei Wang(王欣伟), and Guo-Ping Jiang(蒋国平)
Chin. Phys. B, 2024, 33 (**4**): 040205. DOI: 10.1088/1674-1056/ad20d7

Intralayer structure reconstruction of general weighted output-coupling multilayer complex networks

Xinwei Wang(王欣伟)[1,2], Yayong Wu(吴亚勇)[1,2], Ying Zheng(郑颖)[1,2], and Guo-Ping Jiang(蒋国平)[1,2,†]

[1] *College of Automation and College of Artificial Intelligence, Nanjing University of Posts and Telecommunications, Nanjing* 210023, *China*
[2] *Jiangsu Engineering Laboratory for IOT Intelligent Robots (IOTRobot), Nanjing* 210023, *China*

(Received 22 May 2025; revised manuscript received 8 July 2025; accepted manuscript online 18 July 2025)

Multilayer complex dynamical networks, characterized by the intricate topological connections and diverse hierarchical structures, present significant challenges in determining complete structural configurations due to the unique functional attributes and interaction patterns inherent to different layers. This paper addresses the critical question of whether structural information from a known layer can be used to reconstruct the unknown intralayer structure of a target layer within general weighted output-coupling multilayer networks. Building upon the generalized synchronization principle, we propose an innovative reconstruction method that incorporates two essential components in the design of structure observers, the cross-layer coupling modulator and the structural divergence term. A key advantage of the proposed reconstruction method lies in its flexibility to freely designate both the unknown target layer and the known reference layer from the general weighted output-coupling multilayer network. The reduced dependency on full-state observability enables more deployment in engineering applications with partial measurements. Numerical simulations are conducted to validate the effectiveness of the proposed structure reconstruction method.

Keywords: multilayer network, structure reconstruction, cross-layer coupling modulator, output coupling

PACS: 02.30.Yy, 07.05.Dz, 05.45.Xt

DOI: 10.1088/1674-1056/adf180 **CSTR:** 32038.14.CPB.adf180

1. Introduction

Modern interconnected systems exhibit complex dynamical behaviors across multiple domains, ranging from biological neural networks[1,2] to critical infrastructure grids[3,4] and social communication networks.[5,6] Deciphering structural configurations and operational principles of these networks provides fundamental insights into collective phenomena that individual components cannot exhibit.[7,8] From engineering perspectives, complete network mapping proves essential for optimizing data transmission pathways,[9] streamlining supply chain logistics,[10] and maintaining energy distribution stability.[11]

The current research employs diverse methods for structure reconstruction. The graph-based approaches adopt signal processing[12,13] and neural architectures,[14,15] while statistical methods utilize Bayesian probability models[16,17] and causal relationship analysis.[18,19] Sparse reconstruction techniques like compressed sensing[20,21] demonstrate particular effectiveness in handling high-dimensional networks. Recent structure reconstruction algorithms have expanded capabilities to linear dynamics via Lyapunov equation formulations[22] and nonlinear agent systems through global convergence properties.[23] A motif-driven hypergraph construction method was studied to enhance graph structure learning.[24] By inserting motifs as hypernodes into the original graph to form a heterogeneous network, it handled incomplete information to facilitate the structure reconstruction. A network reconstruction method was presented for binary-state dynamical systems using generalized statistical inference.[25] Based on observational data, the approach employed statistical inference principles and the expectation–maximization algorithms to deduce network structures. The topology identification of weighted networks was addressed using binary time series generated by propagation dynamics.[26] It utilized the observed binary-state dynamics to reconstruct network topologies via maximum likelihood estimation and regularization optimization. The drive-response framework[27,31–34] has become widely adopted for constructing auxiliary observation networks, with progress in handling real-world interference factors like time delays,[27,28] stochastic noise,[29,30] undetected nodes,[31] and dynamics uncertainties.[32,33] Emerging frontiers incorporate intermittent control,[34] fractional-order domain[33,35] and partial topology detection,[36,37] enhancing the practical applicability of structure reconstruction for complex dynamical networks.

Many complex dynamical networks in the real world exhibit multilayer architectures where interdependent subsystems interact through cross-layer couplings. In such networks, interactions between different layers can give rise to new dynamical behaviors,[38] and the structure reconstruction for multilayer complex dynamical networks presents unique

[†]Corresponding author. E-mail: jianggp@njupt.edu.cn

© 2026 Chinese Physical Society and IOP Publishing Ltd. All rights, including for text and data mining, AI training, and similar technologies, are reserved.

complexities.[39] Constructing the drive-response system facilitates the topology identification of multilayer networks with unidirectional interlayer coupling,[40] with chaotic signal injections overcoming linear independence constraints.[41] Furthermore, an enhanced synchronization-based topology identification method was studied, which eliminates the need for the linear independence condition.[42] The method involved constructing a drive network with isolated nodes and allowing an estimation matrix to accurately identify the unknown structural matrix. While compressed sensing remains common for its computational efficiency,[43,44] specialized reconstruction techniques have been developed for stochastic hybrid multilayer networks[45] and delayed output-coupling multiplex systems.[46] The output coupling mechanism exhibits enhanced operational feasibility in complex networks by using low-dimensional observable network responses rather than relying on direct and full access to node state variables.[47] It enables robust deployment in engineering implementations constrained by partial measurements.[48]

In real-world multilayer networks, practical implementations of the cross-layer inference capability hold considerable significance. For instance, in social networks, which have multilayer structures, there are visible reference layers like friendship networks, where connections between users are easily observable through interactions such as friend requests. There are also hidden target layers, like user preference networks, where connections reflecting shared interests are indirect and hard to measure. We treat the friendship network as the known layer, and the user preference network as the target layer, which we need to reconstruct to understand user behavior patterns relying on low-dimensional outputs like likes or shares. It respects privacy constraints on social platforms and efficiently reconstructs hidden preference structures without requiring complete user information. In power grids, which feature a hierarchical multilayer structure, the well-monitored transmission layers have known connections between substations through supervisory control and data acquisition systems. In contrast, the distribution layers, with feeder lines between substations, are often inadequately sensed due to cost limitations. The transmission layer is designated as the known layer and the distribution layer as the target layer, aiming to reconstruct the connections in the distribution layer to ensure stable energy distribution. However, a previous study[49] explored reconstructing unknown structures in two-layer multiplex networks by using the topology of one known layer as prior information. This method primarily focuses on adjacent layer interactions, neglecting the interference effects cumulated from non-adjacent layers in multilayer networks, which may fall short in more general multilayer network architectures. When identifying non-neighboring layers, coupling effects from intermediate or unrelated layers introduce cumulative interference that disrupts structure observer designs relying solely on direct interlayer interactions.

Based on the above discussion, the paper introduces a generalized method for intralayer structure reconstruction in general weighted output-coupling multilayer complex dynamical networks. An improved structure observer incorporates two key terms: a cross-layer coupling modulator to account for the influence of non-neighboring layers and a structural divergence term to quantify the structural disparity between layers. By leveraging the simpler, more accessible structure of one layer, the adaptive observer, grounded in generalized synchronization principles, reconstructs the structure of a more complex and unknown layer while enabling real-time monitoring of sudden structural changes. The advantages of the proposed intralayer structure reconstruction method against existing major methods are presented in Table 1.

Table 1. Comparisons of major methods of intralayer structure reconstruction.

Feature	Ref. [49]	Our method
Network scope	2-layer	M-layer, $M \geq 2$
Layer interactions	adjacent layers only	non-adjacent layers (cross-layer)
Coupling patterns	full-state coupling (n-dimensional)	low-dimensional output coupling (scalar)
Coupling handling	direct interlayer coupling (adjacent)	cross-layer modulator Ω_3
Target/reference layers	fixed (adjacent layers)	arbitrarily selected
Flexibility	low	high

The main contributions are summarized in the following.

(i) Our method addresses the challenge of reconstructing the intralayer structure between non-neighboring layers in general weighted output-coupling multilayer networks, which is a more complex, general and efficient scenario than the two-layer multiplex network setup in Ref. [49]. Compared with prior work,[49] the proposed reconstruction method accounts for the cross-layer coupling interactions, which are critical for accurately reconstructing unknown layers in real multilayer networks where non-neighboring layers rarely function in isolation. The generality of our method enhances the applicability to diverse domains, from multilayer social networks to hierarchical power grids, etc.

(ii) Our method offers great flexibility in selecting reference layers based on data accessibility and operational constraints when targeting any other layer for reconstruction. By

integrating the cross-layer coupling modulator and structural divergence term, the proposed method enables layers with distinct intralayer structures to achieve the generalized synchronization, ensuring the structure reconstruction across heterogeneous layers in the general weighted output-coupling multilayer networks.

(iii) Our method is aimed at reconstructing the intralayer structure in the general weighted multilayer networks featuring output coupling. Unlike state coupling, output coupling mechanism demonstrates superior practicality in complex networks, which operates solely through the lower-dimensional observable network responses, rather than the direct and full access to node state variables. The reduced dependency on full-state observability enables wide deployment in engineering applications with partial measurements or privacy constraints.

The remainder of this paper is organized as follows. Section 2 introduces the necessary preliminaries and presents the problem formulation. Section 3 details the main results on intralayer structure reconstruction for general weighted output-coupling multilayer networks. The effectiveness of the proposed reconstruction method is validated through numerical simulations in Section 4. Section 5 concludes this paper.

The notation of this paper is described in the following. I represents the identity matrix with appropriate dimensions, $\mathrm{diag}\{x_1,x_2,\ldots,x_n\}$ is a diagonal matrix formed by matrices $x_1,x_2,\ldots,x_n$, $\otimes$ denotes the Kronecker product, and $\|\cdot\|$ denotes the Euclidean norm.

2. Problem formulation

Consider a general output-coupling multilayer complex dynamical network in which the nodes in different layers are coupled in one-to-one manner. The network features an M-layer structure, where each layer consists of N nonidentical nodes, which is described as follows:

$$\begin{cases} \dot{x}_i^{(Q)}(t) = f_i^{(Q)}\left(x_i^{(Q)}(t)\right) + \varepsilon \sum\limits_{j=1}^{N} d_{ij}^{(Q)} L y_j^{(Q)}(t) \\ \qquad\qquad + \varepsilon \sum\limits_{P=1}^{M} d_i^{(Q)(P)} L y_i^{(P)}(t), \\ y_i^{(Q)}(t) = H x_i^{(Q)}(t), \end{cases} \tag{1}$$

where $i=1,2,\ldots,N$, $Q=1,2,\ldots,M$. In this model, $x_i^{(Q)}(t) = \left(x_{i1}^{(Q)}(t),x_{i2}^{(Q)}(t),\ldots,x_{in}^{(Q)}(t)\right)^{\mathrm{T}} \in R^n$ is the n-dimensional state vector of the i-th node in the Q-th layer. $y_i^{(Q)}(t) = \left(y_{i1}^{(Q)}(t),y_{i2}^{(Q)}(t),\ldots,y_{im}^{(Q)}(t)\right)^{\mathrm{T}} \in R^m$ is the m-dimensional output variable of the i-th node in the Q-th layer. $f_i^{(Q)}(\cdot): R \times R^n \to R^n$ is a continuously differentiable vector function which characterizes the dynamical behavior of the i-th node in the Q-th layer. ε denotes the coupling strengths associated with both the intralayer structure within each layer and the interlayer structure between different layers. The inner output-coupling matrix is set as $L \in R^{n\times m}$, which describes the coupling pattern of output components between different nodes. $H \in R^{m\times n}$ is the output matrix. When $m=1$, the output variable $y_i^{(Q)}(t)$ becomes actually a scalar that denotes the linear combination of state components of $x_i^{(Q)}(t)$. The weighted interlayer configuration matrix is denoted as $D^{\mathrm{inter}} = \left(d_i^{(Q)(P)}\right)_{M\times M} \in R^{M\times M}$. If there is a non-zero edge connecting node $i^{(P)}$ to node $i^{(Q)}$, then $d_i^{(Q)(P)} \neq 0$; otherwise, $d_i^{(Q)(P)} = 0$. Assume that the diagonal elements $\left\{d_i^{(Q)(Q)}\right\}_{Q=1}^{M}$ of D^{inter} satisfy $d_i^{(Q)(Q)} = -\sum_{P=1,P\neq Q}^{M} d_i^{(Q)(P)}$, a common setup for the adjacency matrix in complex dynamical networks. The weighted intralayer structural matrix is $D^{(Q)} = \left(d_{ij}^{(Q)}\right)_{N\times N} \in R^{N\times N}$, which indicates the coupling relationship among nodes within the Q-th layer. If there is a non-zero edge from node $j^{(Q)}$ to node $i^{(Q)}$, then $d_{ij}^{(Q)} \neq 0$; otherwise, $d_{ij}^{(Q)} = 0$. Likewise, let the diagonal elements $\left\{d_{ii}^{(Q)}\right\}_{i=1}^{N}$ of $D^{(Q)}$ satisfy $d_{ii}^{(Q)} = -\sum_{j=1,j\neq i}^{N} d_{ij}^{(Q)}$. It is important to note that neither D^{inter} and $\left\{D^{(Q)}\right\}_{Q=1}^{M}$ are not required to be irreducible, symmetric or diffusive. Employing the output coupling approach for node interaction obviates the necessity of accessing the full state vector of nodes. It allows for easier data acquisition and measurement, enhancing the efficiency of node coupling communication, which improves substantially the operational feasibility.

Most existing structure reconstruction methods for multilayer complex dynamical networks rely on constructing a large-scale auxiliary network. This approach, however, inherently incurs high computational costs. Reconstructing the full structure of a multilayer network is often challenging. Nevertheless, certain layers may be more accessible to measurement or prior knowledge. In this paper, we leverage the structural information of a known layer to reconstruct an unknown layer, offering a more feasible solution for analyzing multilayer networks with partial output information availability.

For the proposed structure reconstruction method, we randomly select the K-th layer from the multilayer complex dynamical network Eq. (1). With its structure assumed unknown, we treat the K-th layer as the drive network, which is shown in Eq. (2). Next, we randomly choose the R-th layer. Given its a-priori known structure, we treat the R-th layer as the response network, which is shown in Eq. (3).

$$\begin{cases} \dot{x}_i^{(K)}(t) = f_i\left(x_i^{(K)}(t)\right) + \varepsilon \sum\limits_{j=1}^{N} d_{ij}^{(K)} L y_j^{(K)}(t) \\ \qquad\qquad + \varepsilon \sum\limits_{P=1}^{M} d_i^{(K)(P)} L y_i^{(P)}(t), \\ y_i^{(K)}(t) = H x_i^{(K)}(t), \end{cases} \tag{2}$$

$$
\begin{cases}
\dot{x}_i^{(R)}(t) = f_i\left(x_i^{(R)}(t)\right) + \varepsilon \sum_{j=1}^{N} d_{ij}^{(R)} L y_j^{(R)}(t) \\
\qquad\qquad + \varepsilon \sum_{P=1}^{M} d_i^{(R)(P)} L y_i^{(P)}(t) + u_i(t), \\
y_i^{(R)}(t) = H x_i^{(R)}(t), \\
u_i(t) = \Omega_1 + \Omega_2 + \Omega_3, \\
\Omega_1 = -k_i(t)\left(x_i^{(R)}(t) - x_i^{(K)}(t)\right), \\
\Omega_2 = -\varepsilon \sum_{j=1}^{N} g_{ij}(t) L y_j^{(R)}(t), \\
\Omega_3 = \varepsilon \sum_{\substack{P=1 \\ P\neq K \\ P\neq R}}^{M} \left(d_i^{(K)(P)} - d_i^{(R)(P)}\right) LH\left(x_i^{(P)}(t) - x_i^{(K)}(t)\right),
\end{cases}
\tag{3}
$$

where $\left\{x_i^{(K)}(t)\right\}_{i=1}^{N}$ are the state vectors of nodes in the K-th layer with unknown structural matrix $D^{(K)} = \left(d_{ij}^{(K)}\right)_{N\times N}$. $\left\{x_i^{(R)}(t)\right\}_{i=1}^{N}$ are the state vectors of nodes in the R-th layer, with known structural matrix $D^{(R)} = \left(d_{ij}^{(R)}\right)_{N\times N}$. For simplicity, $\left\{f_i^{(R)}(\cdot)\right\}_{Q=1}^{M}$ are set as the same dynamical vector function $f_i(\cdot)$. Let $m = 1$, $y_i^{(K)}(t)$ and $y_i^{(R)}(t)$ are the output scalars of the i-th node in the K-th layer and the R-th layer respectively. In Eq. (3), $u_i(t)$ is the structure observer applied to the i-th node of the response network. It consists of the adaptive feedback term Ω_1, the structural divergence term Ω_2, the cross-layer coupling modulator Ω_3. $k_i \in R$ is adaptive feedback gain. Ω_2 is introduced for the structure reconstruction. Our reconstruction method, to be developed below, offers the capability to arbitrarily choose the target layer and the known layer from the output-coupling multilayer complex dynamical network, which shows a high level of flexibility and adaptability. The known $D^{(R)}$ is different from the unknown target $D^{(K)}$, and the exact divergence between them is given by $G^* = D^{(R)} - D^{(K)}$, which remains unknown initially. The element $g_{ij}(t)$ of $G \in R^{N\times N}$ in Ω_2 can be arbitrarily initialized. In order to reconstruct the target matrix $D^{(K)}$ of the drive network Eq. (2) using the known $D^{(R)}$, a suitable update law for G must be designed to ensure its convergence to G^* as the generalized synchronization between the drive and the response networks is gradually achieved. Interlayer interactions within multilayer networks significantly increase the complexity of designing reconstruction algorithms. Notably, even in the absence of direct coupling between two adjacent layers, other layers can induce cross-layer coupling effects through interlayer interactions. When reconstructing the unknown $D^{(K)}$ of the drive network Eq. (2) using the arbitrarily-chosen response network Eq. (3), the drive network Eq. (2) is inevitably influenced by the interlayer interactions from other layers, significantly impacting the design of the structure observer $u_i(t)$, which is illustrated in Fig. 1.

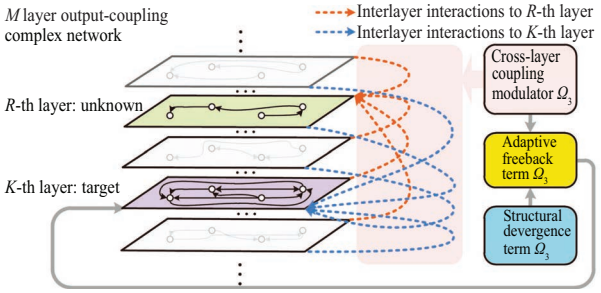


Fig. 1. The structure observer $u_i(t)$ is designed with the structural divergence term Ω_2 and the cross-layer coupling modulator Ω_3.

The mixture of direct and cross-layer couplings presents the main challenge in designing structure observers for output-coupling multilayer networks, which will be further discussed in the following.

Remark 1 In the general weighted output-coupling multilayer complex dynamical network, the cross-layer coupling modulator Ω_3 has been introduced to address the problem of mitigating the cumulative interlayer influence and reconstructing unknown intralayer structure of a given layer by leveraging information from another known and relatively simple layer. A key advantage of this approach lies in its ability to account for coupling effects originating from non-adjacent layers in the output-coupling multilayer network. This feature distinguishes it from methods that merely extend the structure reconstruction techniques for two-layer multiplex networks,[49] as those straightforward extensions fail to incorporate such cross-layer interlayer interactions.

Remark 2 The reconstruction of the structural divergence matrix G is critical, as it enables the reconstruction of complex, unknown intralayer structure by leveraging information from simple, known, and arbitrarily selected layer from the multilayer network. The initial value of each element $g_{ij}(t)$ of $G \in R^{N\times N}$ in Ω_2 can be arbitrarily set. Given that the structures $D^{(K)}$ and $D^{(R)}$ of drive and response networks typically differ, sole reliance on $D^{(R)}$ proves insufficient for reconstructing $D^{(K)}$. Consequently, introducing the structural divergence term Ω_2 becomes necessary to estimate difference between $D^{(K)}$ and $D^{(R)}$ through the generalized synchronization of drive and response networks.

Remark 3 The interlayer weight $d_i^{(K)(P)}$ and $d_i^{(R)(P)}$ in the cross-layer coupling modulator Ω_3 are assumed to be known a priori, which exists reasonably in the real world. For example, in the transmission layer of power grids, high-voltage network transports bulk electricity between power plants, substations, and major load centers over long distances. In the distribution layer, low-voltage network delivering electricity from substations to end-users. The interlayer connections, representing power flows and exchange of control signals, are measurable

via substation telemetry or managed actively by grid operators. This indicates that in a multilayer power network, the interlayer coupling interaction can be clearly known or obtained in advance.

Let $e_i(t) = x_i^{(R)}(t) - x_i^{(K)}(t)$. Through the drive network Eq. (2) and the response network Eq. (3), the error dynamical network can be obtained as follows:

$$
\begin{aligned}
\dot{e}_i(t) &= \dot{x}_i^{(R)}(t) - \dot{x}_i^{(K)}(t) \\
&= f_i\left(x_i^{(R)}(t)\right) - f_i\left(x_i^{(K)}(t)\right) + \varepsilon \sum_{j=1}^{N} d_{ij}^{(R)} Ly_j^{(R)}(t) + \varepsilon \sum_{P=1}^{M} d_i^{(R)(P)} Ly_i^{(P)}(t) \\
&\quad - \varepsilon \sum_{j=1}^{N} d_{ij}^{(K)} Ly_j^{(K)}(t) - \varepsilon \sum_{P=1}^{M} d_i^{(K)(P)} Ly_i^{(P)}(t) - k_i(t) e_i(t) - \varepsilon \sum_{j=1}^{N} g_{ij}(t) Ly_j^{(R)}(t) \\
&\quad + \varepsilon \sum_{\substack{P=1 \\ P\neq K \\ P\neq R}}^{M} \left(d_i^{(K)(P)} - d_i^{(R)(P)}\right) LH\left(x_i^{(P)}(t) - x_i^{(K)}(t)\right) \\
&= f_i\left(x_i^{(R)}(t)\right) - f_i\left(x_i^{(K)}(t)\right) + \varepsilon \sum_{j=1}^{N} \left(d_{ij}^{(R)} - g_{ij}(t)\right) Ly_j^{(R)}(t) - \varepsilon \sum_{j=1}^{N} d_{ij}^{(K)} Ly_j^{(K)}(t) \\
&\quad + \varepsilon \left(d_i^{(R)(R)} - d_i^{(K)(R)}\right) Ly_i^{(R)}(t) - \varepsilon \left(d_i^{(K)(K)} - d_i^{(R)(K)}\right) Ly_i^{(K)}(t) - k_i(t) e_i(t) + \varepsilon \sum_{\substack{P=1 \\ P\neq K \\ P\neq R}}^{M} d_i^{(R)(P)} Ly_i^{(P)}(t) - \varepsilon \sum_{\substack{P=1 \\ P\neq K \\ P\neq R}}^{M} d_i^{(K)(P)} Ly_i^{(P)}(t) \\
&\quad + \varepsilon \sum_{\substack{P=1 \\ P\neq K \\ P\neq R}}^{M} \left(d_i^{(K)(P)} - d_i^{(R)(P)}\right) LH\left(x_i^{(P)}(t) - x_i^{(K)}(t)\right) \\
&= f_i\left(x_i^{(R)}(t)\right) - f_i\left(x_i^{(K)}(t)\right) + \varepsilon \sum_{j=1}^{N} \left(d_{ij}^{(R)} - g_{ij}(t)\right) Ly_j^{(R)}(t) - \varepsilon \sum_{j=1}^{N} d_{ij}^{(K)} Ly_j^{(K)}(t) \\
&\quad + \varepsilon \sum_{\substack{P=1 \\ P\neq K \\ P\neq R}}^{M} \left(d_i^{(K)(P)} - d_i^{(R)(P)}\right) LH\left(x_i^{(P)}(t) - x_i^{(K)}(t)\right) - k_i(t) e_i(t) + \Phi,
\end{aligned} \tag{4}
$$

where

$$
\begin{aligned}
\Phi &= \varepsilon \left(d_i^{(R)(R)} - d_i^{(K)(R)}\right) Ly_i^{(R)}(t) \\
&\quad - \varepsilon \left(d_i^{(K)(K)} - d_i^{(R)(K)}\right) Ly_i^{(K)}(t) \\
&\quad + \varepsilon \sum_{\substack{P=1 \\ P\neq K \\ P\neq R}}^{M} d_i^{(R)(P)} Ly_i^{(P)}(t) - \varepsilon \sum_{\substack{P=1 \\ P\neq K \\ P\neq R}}^{M} d_i^{(K)(P)} Ly_i^{(P)}(t)
\end{aligned}
$$

Following the above definition of D^{inter}, one obtains

$$
\sum_{P=1}^{M} d_i^{(K)(P)} = \sum_{P=1}^{M} d_i^{(R)(P)} = 0. \tag{5}
$$

From the two summation terms $\sum_{P=1}^{M} d_i^{(K)(P)}$ and $\sum_{P=1}^{M} d_i^{(R)(P)}$ in Eq. (5), extracting the K-th and R-th terms respectively yields

$$
\begin{aligned}
d_i^{(K)(K)} + d_i^{(K)(R)} + \sum_{\substack{P=1 \\ P\neq K \\ P\neq R}}^{M} d_i^{(K)(P)} &= d_i^{(R)(K)} + d_i^{(R)(R)} \\
&\quad + \sum_{\substack{P=1 \\ P\neq K \\ P\neq R}}^{M} d_i^{(R)(P)} = 0,
\end{aligned} \tag{6}
$$

$$
d_i^{(R)(R)} + d_i^{(R)(K)} = -\sum_{\substack{P=1 \\ P\neq K \\ P\neq R}}^{M} d_i^{(R)(P)}, \tag{7}
$$

$$
d_i^{(K)(K)} + d_i^{(K)(R)} = -\sum_{\substack{P=1 \\ P\neq K \\ P\neq R}}^{M} d_i^{(K)(P)}. \tag{8}
$$

By subtracting Eq. (8) from Eq. (7) and rearranging the terms, one gets

$$
\left(d_i^{(R)(R)} + d_i^{(R)(K)}\right) - \left(d_i^{(K)(K)} + d_i^{(K)(R)}\right) = \left(d_i^{(R)(R)} - d_i^{(K)(R)}\right) - \left(d_i^{(K)(K)} - d_i^{(R)(K)}\right) = \sum_{\substack{P=1 \\ P\neq K \\ P\neq R}}^{M} \left(d_i^{(K)(P)} - d_i^{(R)(P)}\right). \tag{9}
$$

Let $\Lambda_i = d_i^{(R)(R)} - d_i^{(K)(R)}$, $\Xi_i = d_i^{(K)(K)} - d_i^{(R)(K)}$. Upon inserting Eq. (9) into Φ, one derives

$$\begin{aligned}
\Phi &= \varepsilon\Lambda_i L y_i^{(R)}(t) - \varepsilon\Xi_i L y_i^{(K)}(t) - \varepsilon \sum_{\substack{P=1\\P\neq K\\P\neq R}}^{M} \left(d_i^{(K)(P)} - d_i^{(R)(P)}\right) L y_i^{(P)}(t) \\
&= \varepsilon\Lambda_i L y_i^{(R)}(t) - \varepsilon\Lambda_i L y_i^{(K)}(t) + \varepsilon\Lambda_i L y_i^{(K)}(t) - \varepsilon\Xi_i L y_i^{(K)}(t) \\
&\quad - \varepsilon \sum_{\substack{P=1\\P\neq K\\P\neq R}}^{M} \left(d_i^{(K)(P)} - d_i^{(R)(P)}\right) L y_i^{(P)}(t) \\
&= \varepsilon\Lambda_i L H e_i(t) + \varepsilon\left(\Lambda_i - \Xi_i\right) L y_i^{(K)}(t) - \varepsilon \sum_{\substack{P=1\\P\neq K\\P\neq R}}^{M} \left(d_i^{(K)(P)} - d_i^{(R)(P)}\right) L y_i^{(P)}(t) \\
&= \varepsilon\Lambda_i L H e_i(t) + \varepsilon \sum_{\substack{P=1\\P\neq K\\P\neq R}}^{M} \left(d_i^{(K)(P)} - d_i^{(R)(P)}\right) L H \left(x_i^{(K)}(t) - x_i^{(P)}(t)\right).
\end{aligned} \tag{10}$$

Inserting Eq. (10) into the error dynamical network Eq. (4) and subsequently refining it yields

$$\begin{aligned}
\dot{e}_i(t) &= f_i\left(x_i^{(R)}(t)\right) - f_i\left(x_i^{(K)}(t)\right) + \varepsilon \sum_{j=1}^{N} \left(d_{ij}^{(R)} - g_{ij}(t)\right) L y_j^{(R)}(t) - \varepsilon \sum_{j=1}^{N} d_{ij}^{(K)} L y_j^{(K)}(t) \\
&\quad + \varepsilon \sum_{\substack{P=1\\P\neq K\\P\neq R}}^{M} \left(d_i^{(K)(P)} - d_i^{(R)(P)}\right) L H \left(x_i^{(P)}(t) - x_i^{(K)}(t)\right) - k_i(t) e_i(t) + \Phi \\
&= f_i\left(x_i^{(R)}(t)\right) - f_i\left(x_i^{(K)}(t)\right) + \varepsilon \sum_{j=1}^{N} \left(d_{ij}^{(R)} - g_{ij}(t)\right) L y_j^{(R)}(t) - \varepsilon \sum_{j=1}^{N} d_{ij}^{(K)} L y_j^{(K)}(t) \\
&\quad + \varepsilon \sum_{\substack{P=1\\P\neq K\\P\neq R}}^{M} \left(d_i^{(K)(P)} - d_i^{(R)(P)}\right) L H \left(x_i^{(P)}(t) - x_i^{(K)}(t)\right) - k_i(t) e_i(t) + \varepsilon\Lambda_i L H e_i(t) \\
&\quad + \varepsilon \sum_{\substack{P=1\\P\neq K\\P\neq R}}^{M} \left(d_i^{(K)(P)} - d_i^{(R)(P)}\right) L H \left(x_i^{(K)}(t) - x_i^{(P)}(t)\right) \\
&= f_i\left(x_i^{(R)}(t)\right) - f_i\left(x_i^{(K)}(t)\right) - k_i(t) e_i(t) + \varepsilon\Lambda_i L H e_i(t) \\
&\quad + \varepsilon \sum_{j=1}^{N} \left(d_{ij}^{(R)} - g_{ij}(t)\right) L y_j^{(R)}(t) - \varepsilon \sum_{j=1}^{N} d_{ij}^{(K)} L y_j^{(K)}(t) \\
&= f_i\left(x_i^{(R)}(t)\right) - f_i\left(x_i^{(K)}(t)\right) - k_i(t) e_i(t) + \varepsilon \sum_{j=1}^{N} \left(d_{ij}^{(R)} - g_{ij}(t)\right) L y_j^{(R)}(t) \\
&\quad - \varepsilon \sum_{j=1}^{N} d_{ij}^{(K)} L y_j^{(R)}(t) + \varepsilon \sum_{j=1}^{N} d_{ij}^{(K)} L y_j^{(R)}(t) - \varepsilon \sum_{j=1}^{N} d_{ij}^{(K)} L y_j^{(K)}(t) + \varepsilon\Lambda_i L H e_i(t) \\
&= f_i\left(x_i^{(R)}(t)\right) - f_i\left(x_i^{(K)}(t)\right) - k_i(t) e_i(t) + \varepsilon\Lambda_i L H e_i(t) \\
&\quad + \varepsilon \sum_{j=1}^{N} d_{ij}^{(K)} L H e_j(t) + \varepsilon \sum_{j=1}^{N} \left(d_{ij}^{(R)} - g_{ij}(t) - d_{ij}^{(K)}\right) L y_j^{(R)}(t).
\end{aligned} \tag{11}$$

To prove the stability of the error dynamical network, it is essential to introduce certain assumptions and lemmas.

Assumption 1 For a smooth nonlinear vector function $f_i(\cdot)$, it is assumed that there exists a positive constant δ such that $f_i(\cdot)$ satisfies the following expression:

$$\|f_i(x(t)) - f_i(y(t))\| \leq \delta \|x(t) - y(t)\| \tag{12}$$

for $\forall\, x(t), y(t) \in R^n$, $i = 1, 2, \ldots, N$.

Assumption 2 For $i,j \in \{1,2,\ldots,N\}$, all $\left\{LHx_j^{(K)}(t)\right\}_{j=1}^{N}$ along the orbits $\left\{x_i^{(K)}(t)\right\}_{i=1}^{N}$ on the synchronization manifold $\left\{x_i^{(R)} = x_i^{(K)}\right\}_{i=1}^{N}$ are linearly independent.[41,42,46,49]

Lemma 1 (Barbălat Lemma) Assume that $x(t)$ satisfies square integrability, i.e., $\lim_{t\to\infty}\int_0^t x^2(\upsilon)\,\mathrm{d}\upsilon < \infty$, and $\dot{x}(t)$ exists and is bounded, then it follows that $\lim_{t\to\infty} x(t) = 0$.[50]

Lemma 2 Suppose that $x(t)$ is differentiable, $\dot{x}(t)$ exhibits Lipschitz continuity, and $\lim_{t\to\infty} x(t) = 0$, then it follows that $\lim_{t\to\infty}\dot{x}(t) = 0$.

3. Main results

In this section, a structure reconstruction method is developed for the aforementioned weighted output-coupling multilayer networks featuring distinct intralayer structures. The proposed reconstruction method leverages the generalized synchronization between the drive and response networks, utilizing the simple intralayer structural information from the known layer.

Theorem 1 Suppose that Assumption 1 and Assumption 2 hold, by employing the reconstruction update law

$$\dot{g}_{ij}(t) = e_i^{\mathrm{T}}(t)Ly_j^{(R)}(t), \tag{13}$$

the adaptive control law

$$\dot{k}_i(t) = \beta_i \left\|e_i(t)\right\|^2, \tag{14}$$

and the feedback structure observer

$$u_i(t) = -k_i(t)\left(x_i^{(R)}(t) - x_i^{(K)}(t)\right) - \varepsilon\sum_{j=1}^{N} g_{ij}(t)Ly_j^{(R)}(t) + \varepsilon\sum_{\substack{P=1\\P\neq K\\P\neq R}}^{M}\left(d_i^{(K)(P)} - d_i^{(R)(P)}\right)LH\left(x_i^{(P)}(t) - x_i^{(K)}(t)\right), \tag{15}$$

the error dynamical network Eq. (4) will asymptotically converge to the zero equilibrium point, where $\beta_i > 0$. Then, asymptotic synchronization between the response network Eq. (3) and the drive network Eq. (2) will be achieved. Meanwhile, the intralayer structure $D^{(K)}$ of the K-th layer, i.e., the drive network Eq. (2), will be reconstructed by leveraging the structural divergence matrix G and the known structural matrix $D^{(R)}$ of the R-th layer, i.e., the response network Eq. (3).

Proof Construct a non-negative Lyapunov function $V(t)$ as follows:

$$V(t) = \frac{1}{2}\sum_{i=1}^{N} e_i^{\mathrm{T}}(t)e_i(t) + \frac{1}{2}\varepsilon\sum_{i=1}^{N}\sum_{j=1}^{N}\left(d_{ij}^{(R)} - d_{ij}^{(K)} - g_{ij}(t)\right)^2 + \frac{1}{2}\sum_{i=1}^{N}\frac{1}{\beta_i}\left(k_i(t) - k^*\right)^2. \tag{16}$$

By integrating the feedback structure observer Eq. (15), the derivative of the Lyapunov function V, denoted as $\dot{V}$, is determined in the following:

$$\begin{aligned}
\dot{V}(t) &= \sum_{i=1}^{N} e_i^{\mathrm{T}}(t)\dot{e}_i(t) + \sum_{i=1}^{N}\frac{1}{\beta_i}\left(k_i(t) - k^*\right)\dot{k}_i(t) - \varepsilon\sum_{i=1}^{N}\sum_{j=1}^{N}\left(d_{ij}^{(R)} - d_{ij}^{(K)} - g_{ij}(t)\right)\dot{g}_{ij}(t)\\
&= \sum_{i=1}^{N} e_i^{\mathrm{T}}(t)\left(f_i\left(x_i^{(R)}(t)\right) - f_i\left(x_i^{(K)}(t)\right) - k_i(t)e_i(t) + \varepsilon\Lambda_i LHe_i(t)\right)\\
&\quad + \sum_{i=1}^{N} e_i^{\mathrm{T}}(t)\left(\varepsilon\sum_{j=1}^{N}\left(d_{ij}^{(R)} - g_{ij}(t) - d_{ij}^{(K)}\right)Ly_j^{(R)}(t) + \varepsilon\sum_{j=1}^{N} d_{ij}^{(K)}LHe_j(t)\right)\\
&\quad - \varepsilon\sum_{i=1}^{N}\sum_{j=1}^{N}\left(d_{ij}^{(R)} - d_{ij}^{(K)} - g_{ij}\right)\dot{g}_{ij}(t) + \sum_{i=1}^{N}\frac{1}{\beta_i}\left(k_i(t) - k^*\right)\dot{k}_i(t).
\end{aligned} \tag{17}$$

Under Assumption 1 and Assumption 2, substituting the reconstruction update law Eq. (13) and the adaptive control law Eq. (14) into Eq. (17), followed by the linearization of nonlinear terms, yields

$$\begin{aligned}
\dot{V}(t) &= \sum_{i=1}^{N} e_i^{\mathrm{T}}(t)\left(f_i\left(x_i^{(R)}(t)\right) - f_i\left(x_i^{(K)}(t)\right) - k_i(t)e_i(t) + \varepsilon\Lambda_i LHe_i(t)\right)\\
&\quad + \sum_{i=1}^{N} e_i^{\mathrm{T}}(t)\left(\varepsilon\sum_{j=1}^{N}\left(d_{ij}^{(R)} - g_{ij}(t) - d_{ij}^{(K)}\right)Ly_j^{(R)}(t) + \varepsilon\sum_{j=1}^{N} d_{ij}^{(K)}LHe_j(t)\right)\\
&\quad - \varepsilon\sum_{i=1}^{N}\sum_{j=1}^{N}\left(d_{ij}^{(R)} - d_{ij}^{(K)} - g_{ij}(t)\right)\dot{g}_{ij}(t) + \sum_{i=1}^{N}\frac{1}{\beta_i}\left(k_i(t) - k^*\right)\beta_i\left\|e_i(t)\right\|^2
\end{aligned}$$

$$
\begin{aligned}
&\leq \sum_{i=1}^{N} e_i^{\mathrm{T}}(t)\left(\delta e_i(t) - k_i(t)e_i(t) + \varepsilon\Lambda_i LHe_i(t)\right) + \varepsilon\sum_{i=1}^{N}\sum_{j=1}^{N} e_i^{\mathrm{T}}(t)d_{ij}^{(K)}LHe_j(t)\\
&\quad + \sum_{i=1}^{N} k_i(t)\left\|e_i(t)\right\|^2 - \sum_{i=1}^{N} k^*\left\|e_i(t)\right\|^2\\
&= \sum_{i=1}^{N} e_i^{\mathrm{T}}(t)\left(\delta e_i(t) - k_i(t)e_i(t) + \varepsilon\Lambda_i LHe_i(t)\right) + \varepsilon\sum_{i=1}^{N}\sum_{j=1}^{N} e_i^{\mathrm{T}}(t)d_{ij}^{(K)}LHe_j(t)\\
&\quad + \sum_{i=1}^{N} k_i(t)e_i^{\mathrm{T}}(t)e_i(t) - \sum_{i=1}^{N} k^* e_i^{\mathrm{T}}(t)e_i(t)\\
&= (\delta - k^*)\,e^{\mathrm{T}}(t)e(t) + \varepsilon\sum_{i=1}^{N} e_i^{\mathrm{T}}(t)\Lambda_i LHe_i(t) + \varepsilon\sum_{i=1}^{N}\sum_{j=1}^{N} e_i^{\mathrm{T}}(t)d_{ij}^{(K)}LHe_j(t)\\
&= e^{\mathrm{T}}(t)\left((\delta - k^*)I + \varepsilon\left(\Psi\otimes LH\right) + \varepsilon\left(D^{(K)}\otimes LH\right)\right)e(t)\\
&\leq e^{\mathrm{T}}(t)\left(\delta - k^* + \lambda_{\max}\left(\frac{1}{2}\left(\Pi_1 + \Pi_1^{\mathrm{T}}\right)\right) + \lambda_{\max}\left(\frac{1}{2}\left(\Pi_2 + \Pi_2^{\mathrm{T}}\right)\right)\right)e(t),
\end{aligned}
\tag{18}
$$

where $e(t) = \left(e_1^{\mathrm{T}}(t), e_2^{\mathrm{T}}(t), \ldots, e_N^{\mathrm{T}}(t)\right)^{\mathrm{T}}$, $\lambda_{\max}\left(\frac{1}{2}\left(\Pi_1 + \Pi_1^{\mathrm{T}}\right)\right)$ is the maximal eigenvalue of matrix $\frac{1}{2}\left(\Pi_1 + \Pi_1^{\mathrm{T}}\right)$, $\lambda_{\max}\left(\frac{1}{2}\left(\Pi_2 + \Pi_2^{\mathrm{T}}\right)\right)$ is the maximal eigenvalue of matrix $\frac{1}{2}\left(\Pi_2 + \Pi_2^{\mathrm{T}}\right)$, $\Pi_1 = \varepsilon\left(\Psi\otimes LH\right)$, $\Pi_2 = \varepsilon\left(D^{(K)}\otimes LH\right)$, $\Psi = \mathrm{diag}\left(\Lambda_1, \Lambda_2, \ldots, \Lambda_N\right)$.

When $k^* = \delta + \lambda_{\max}\left(\frac{1}{2}\left(\Pi_1 + \Pi_1^{\mathrm{T}}\right)\right) + \lambda_{\max}\left(\frac{1}{2}\left(\Pi_2 + \Pi_2^{\mathrm{T}}\right)\right) + 1$, it follows that $\dot{V}(t) \leq -e^{\mathrm{T}}(t)e(t)$. Given that $\dot{V}(t) \leq 0$, it holds that $0 \leq V(t) \leq V(0)$, implying that $V(t)$ is bounded. From Eq. (16), $e_i(t)$, $k_i(t)$, $\left(d_{ij}^{(R)} - d_{ij}^{(K)} - g_{ij}(t)\right)$ are bounded for $i, j \in \{1, 2, \ldots, N\}$. Notably, $x_i^{(R)}(t)$ and $x_i^{(K)}(t)$ remain bounded for all i. Furthermore, according to Eq. (11), the derivative $\dot{e}_i(t)$ exists and is bounded. By integrating the square of the synchronization error vector $e_i(t)$, it leads to $\lim\limits_{t\to\infty}\int_0^t e^{\mathrm{T}}(\sigma)e(\sigma)\mathrm{d}\sigma \leq -\lim\limits_{t\to\infty}\int_0^t \dot{V}(\sigma)\mathrm{d}\sigma = V(0) - \lim\limits_{t\to\infty} V(t)$. Then, $e_i(t)$ is square-integrable. Since $\dot{e}_i(t)$ exists and is bounded, from Lemma 1, one deduces that $\lim\limits_{t\to\infty} e(t) = 0$, which implies that the drive network Eq. (2) and the response network Eq. (3) achieves synchronization as $t \to \infty$. Given that $\dot{e}_i(t)$ is Lipschitz continuous by Assumption 1 and Eq. (11), one gets $\lim\limits_{t\to\infty}\dot{e}_i(t) = 0$ by applying Lemma 2, and also gets $\lim\limits_{t\to\infty}\varepsilon\sum\limits_{j=1}^{N}\left(d_{ij}^{(R)} - g_{ij}(t) - d_{ij}^{(K)}\right)LHx_j^{(R)}(t) = 0$. Considering $\left(d_{ij}^{(R)} - g_{ij}(t) - d_{ij}^{(K)}\right)$ is bounded, one obtains

$$
\begin{aligned}
&\lim_{t\to\infty}\varepsilon\sum_{j=1}^{N}\left(d_{ij}^{(R)} - g_{ij}(t) - d_{ij}^{(K)}\right)LHx_j^{(R)}(t)\\
&= \lim_{t\to\infty}\varepsilon\sum_{j=1}^{N}\left(d_{ij}^{(R)} - g_{ij}(t) - d_{ij}^{(K)}\right)LH\left(x_j^{(K)}(t) + e_i(t)\right)\\
&= \lim_{t\to\infty}\varepsilon\sum_{j=1}^{N}\left(d_{ij}^{(R)} - g_{ij}(t) - d_{ij}^{(K)}\right)LHx_j^{(K)}(t) + \lim_{t\to\infty}\varepsilon\sum_{j=1}^{N}\left(d_{ij}^{(R)} - g_{ij}(t) - d_{ij}^{(K)}\right)LHe_i(t)\\
&= \lim_{t\to\infty}\varepsilon\sum_{j=1}^{N}\left(d_{ij}^{(R)} - g_{ij}(t) - d_{ij}^{(K)}\right)LHx_j^{(K)}(t) = 0.
\end{aligned}
\tag{19}
$$

From Assumption 2, one concludes that $\lim\limits_{t\to\infty} d_{ij}^{(R)} - g_{ij}(t) - d_{ij}^{(K)} = 0$, i.e., $d_{ij}^{(R)} - g_{ij}(t) \to d_{ij}^{(K)}$ as $t \to \infty$, ensuring that in the general weighted output-coupling multilayer network, the intralayer structure $D^{(K)}$ of the K-th layer can be reconstructed through the structural information $D^{(R)}$ of the R-th layer, even when the two layers exhibit distinct structures. The proof is thus completed.

Remark 4 The coefficient β_i in the adaptive control law $\dot{k}_i = \beta_i\left\|e_i(t)\right\|^2$ governs the convergence rate of synchronization between the drive and response networks. Specifically, increasing the value of β_i accelerates the synchronization process, enabling the two networks to reach a synchronized state more rapidly. Considering practical factors such as implementation costs of structure observers and the significant weakening of control effects in the later stage of the evolution process due to the large reduction in error, there is an optimal value in the consideration of choosing β_i.

4. Numerical simulation

In this section, numerical simulations are conducted to validate the effectiveness of the proposed structure reconstruction method.

The chaotic Lorenz system, which is known for its extreme sensitivity to initial conditions, is chosen to characterize the intricate dynamics of network nodes. It is governed by the following differential equations:

$$\begin{cases} \dot{x}_{i1}(t) = 10\left(x_{i2}(t) - x_{i1}(t)\right), \\ \dot{x}_{i2}(t) = 28x_{i1}(t) - x_{i2}(t) - x_{i1}(t)x_{i3}(t), \\ \dot{x}_{i3}(t) = x_{i1}(t)x_{i2}(t) - \dfrac{8}{3}x_{i3}(t). \end{cases} \tag{20}$$

A simplified weighted output-coupling multilayer complex dynamical network model is established, comprising 5 layers interconnected via one-to-one interlayer interactions and labeled as yellow, green, blue, purple, and red. The second layer (green) is designated as the known and simple layer, while the fourth layer (purple) serves as the unknown target layer whose intralayer structure $D^{(4)}$ requires reconstruction. Only the intralayer structures of the second and the fourth layers are enlarged in Fig. 2 due to space limitation. Also, figures 2 and 3 employ selective blurring with different emphases to visualize clearly the intralayer network structures and interlayer coupling effects.

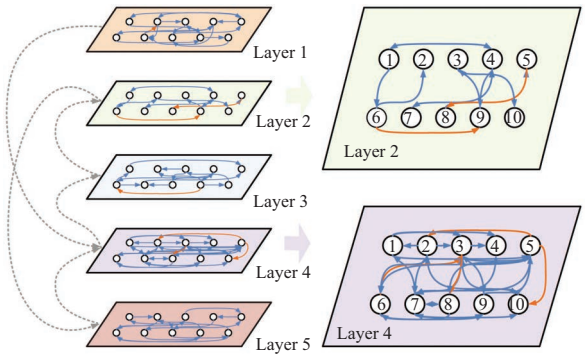


Fig. 2. The weighted output-coupling 5-layer complex dynamical network model.

In Fig. 2, interlayer coupling effects, depicted by dashed lines, are intentionally blurred. Each layer has 10 nodes, and the serial number arrangement of nodes in each layer is identical to that in the enlarged second layer (green) and fourth layer (purple). The blue solid lines denote the coupling with a weight of 1, and the orange solid lines denote the coupling with a weight of 2.

Below are shown the intralayer structural matrices of the known layer $D^{(2)}$ and the target layer $D^{(4)}$:

$$D^{(2)} = \left(d_{ij}^{(2)}\right)_{10\times 10} = \begin{bmatrix} -1 & 0 & 0 & 1 & 0 & 0 & 0 & 0 & 0 & 0 \\ 0 & -1 & 0 & 0 & 0 & 1 & 0 & 0 & 0 & 0 \\ 0 & 0 & -1 & 0 & 0 & 0 & 0 & 0 & 1 & 0 \\ 1 & 0 & 0 & -2 & 0 & 0 & 1 & 0 & 0 & 0 \\ 0 & 0 & 0 & 0 & -1 & 0 & 0 & 1 & 0 & 0 \\ 1 & 0 & 0 & 0 & 0 & -1 & 0 & 0 & 0 & 0 \\ 0 & 0 & 0 & 1 & 0 & 0 & -1 & 0 & 0 & 0 \\ 0 & 0 & 0 & 0 & 2 & 0 & 0 & -2 & 0 & 0 \\ 0 & 0 & 0 & 1 & 0 & 2 & 0 & 0 & -3 & 0 \\ 0 & 0 & 1 & 0 & 0 & 0 & 0 & 0 & 0 & -1 \end{bmatrix},$$

$$D^{(4)} = \left(d_{ij}^{(4)}\right)_{10\times 10} = \begin{bmatrix} -2 & 1 & 0 & 0 & 0 & 0 & 1 & 0 & 0 & 0 \\ 0 & -3 & 0 & 0 & 2 & 0 & 0 & 0 & 0 & 1 \\ 1 & 1 & -7 & 0 & 0 & 2 & 1 & 0 & 1 & 1 \\ 1 & 0 & 1 & -3 & 0 & 0 & 1 & 0 & 0 & 0 \\ 1 & 0 & 1 & 0 & -5 & 0 & 1 & 0 & 1 & 1 \\ 0 & 1 & 0 & 0 & 1 & -3 & 0 & 1 & 0 & 0 \\ 1 & 1 & 1 & 0 & 1 & 0 & -6 & 1 & 0 & 1 \\ 0 & 0 & 2 & 0 & 1 & 0 & 1 & -4 & 0 & 0 \\ 0 & 0 & 1 & 0 & 0 & 1 & 1 & 0 & -3 & 0 \\ 0 & 1 & 0 & 0 & 2 & 0 & 1 & 0 & 0 & -4 \end{bmatrix}.$$

The overall interlayer coupling interactions of the weighted 5-layer network model are demonstrated in Fig. 3.

We abstract the interlayer coupling effects between layers, where nodes in each layer are corresponded one-to-one in sequence, as black dashed lines. It is primarily used to characterize how the interactions between different network layers are distributed. The interlayer configuration matrix D^{inter} is shown below:

$$D^{\text{inter}} = \left(d_i^{(K)(R)}\right)_{5\times 5} = \begin{bmatrix} 0 & 0 & 0 & 0 & 0 \\ 0 & -1 & 1 & 0 & 0 \\ 0 & 0 & -1 & 1 & 0 \\ 1 & 0 & 0 & -2 & 1 \\ 0 & 1 & 0 & 0 & -1 \end{bmatrix}.$$

The second layer is taken as the response network, while the fourth layer is taken as the drive network whose intralayer structural matrix $D^{(4)}$ needs to be reconstructed. For simplic-

ity, assume that $\varepsilon = 0.005$, $H = \begin{bmatrix}1 & 0 & 0\end{bmatrix}$, $L = \begin{bmatrix}1 & 1 & 1\end{bmatrix}^{\mathrm{T}}$. The initial values of all node states in the 5-layer network and the structural difference matrix G are randomly drawn from the range $(0,1)$.

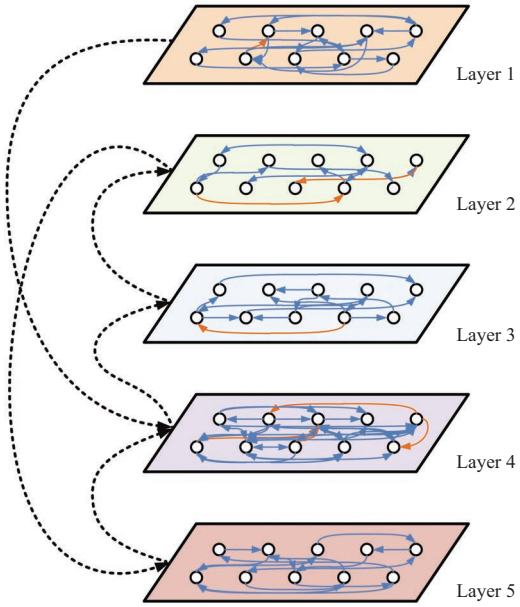


Fig. 3. The overall interlayer coupling interactions of the weighted 5-layer complex dynamical network model.

Figure 4 shows the reconstruction processes of all components in the structural difference matrix G using the reconstruction update law Eq. (13) and the adaptive control law Eq. (14). Based on the reconstruction results of the structural difference matrix G shown in Fig. 4 and the known $D^{(2)}$, the intralayer structure $D^{(4)}$ of the fourth layer is determined according to $D^{(4)} = D^{(2)} - G$. The reconstruction process of the intralayer interactions of each node coupling with others in the fourth layer is shown in Fig. 5. Moreover, the abrupt structure changes can be promptly and accurately detected by the proposed structure reconstruction method.

The error dynamics asymptotically converge to the zero equilibrium as $t \to \infty$, with trajectories detailed in Fig. 6. The dynamic evolution of adaptive feedback gains $\{k_i \mid i = 1,2,\ldots,10\}$ in the structure observers is shown in Fig. 7.

The conducted numerical simulations illustrate the effectiveness and precision of the proposed structure reconstruction method for the weighted 5-layer complex dynamical networks. Specifically, leveraging the reconstruction update law Eq. (13) and the adaptive control law Eq. (14), the intralayer structure $D^{(4)}$ of the fourth layer is successfully reconstructed by the second layer based on the generalized synchronization. Notably, when applied to the weighted multilayer networks with increased node complexity and structure heterogeneity, this approach maintains accuracy and efficiency provided the sufficient conditions defined in Theorem 1 are satisfied, exhibiting robust generalizability.

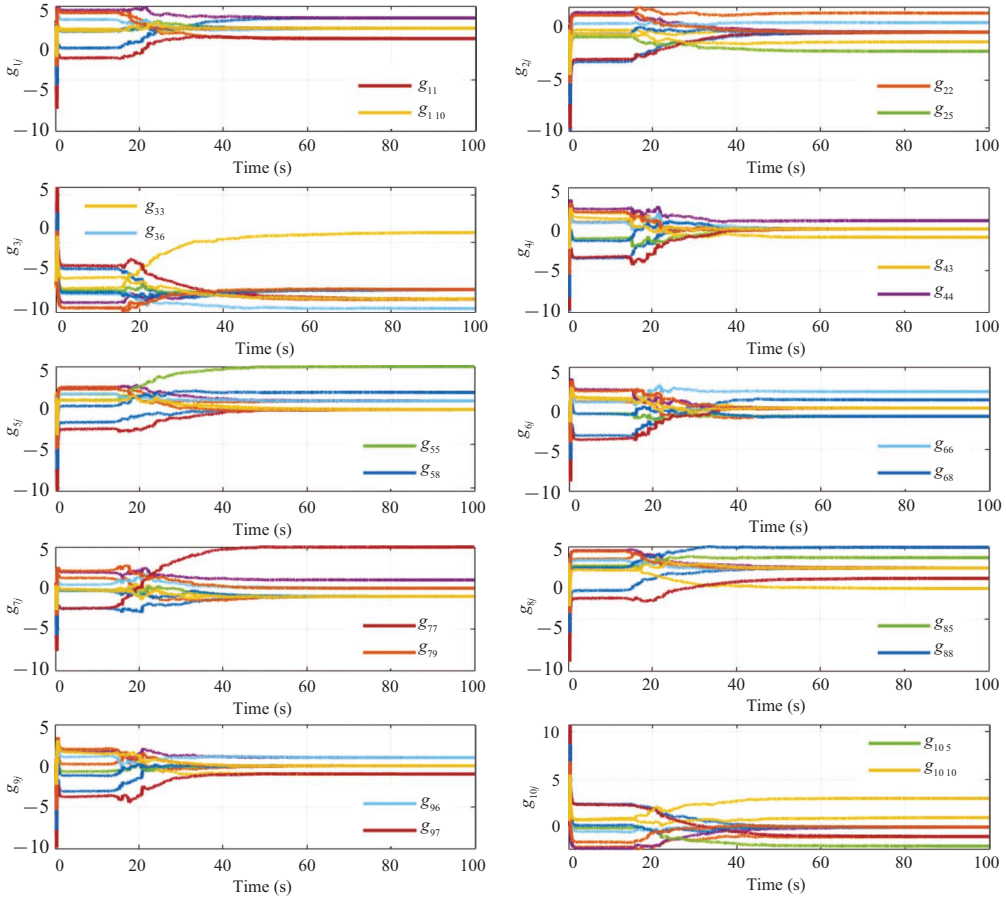


Fig. 4. Reconstruction processes of the structural difference matrix G.

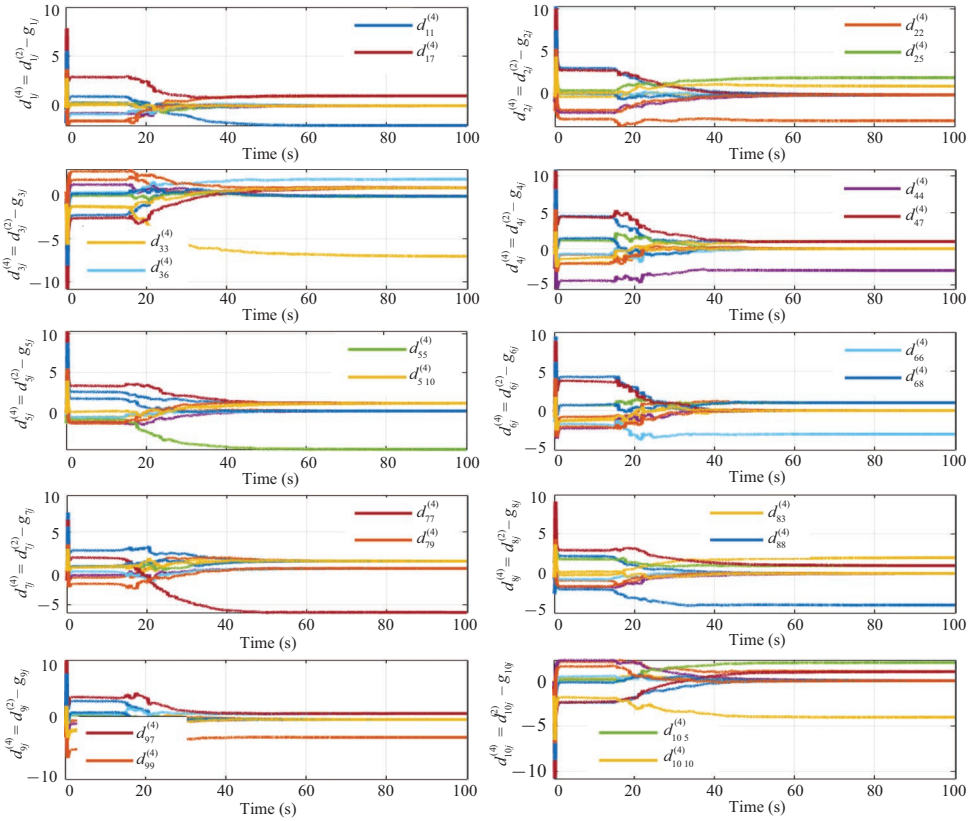


Fig. 5. Reconstruction process of the intralayer structure $D^{(4)}$ of the fourth layer.

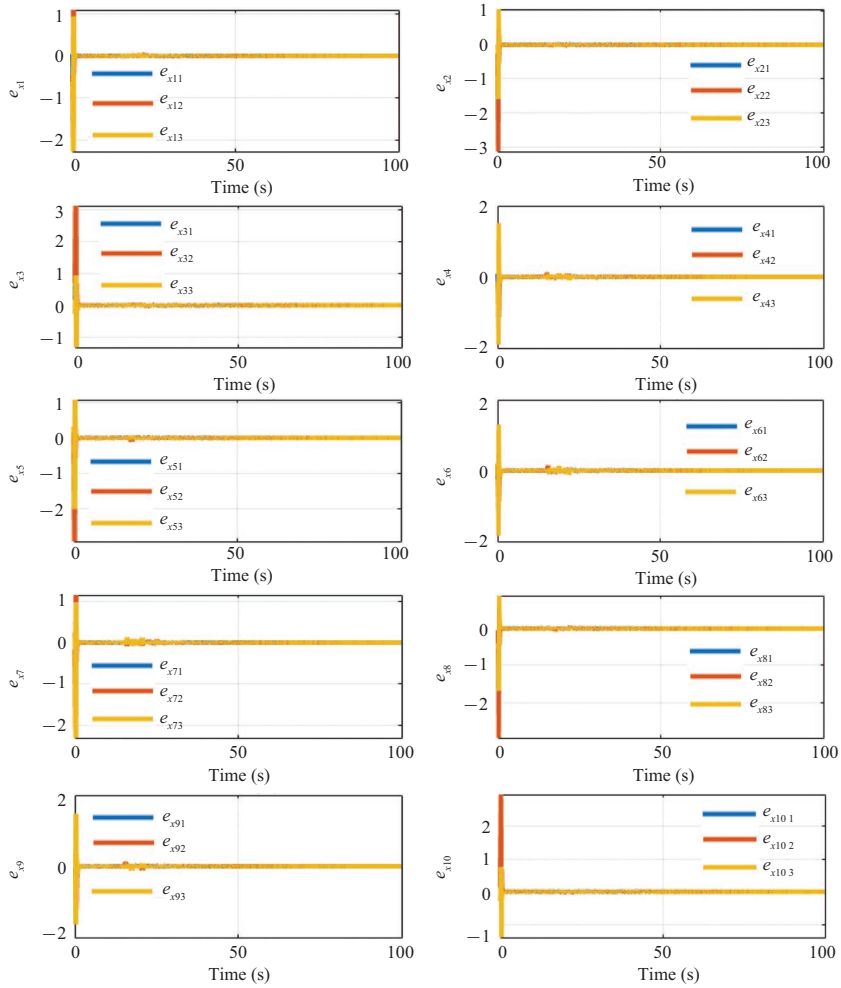


Fig. 6. Error state variables between the second and the fourth layers.

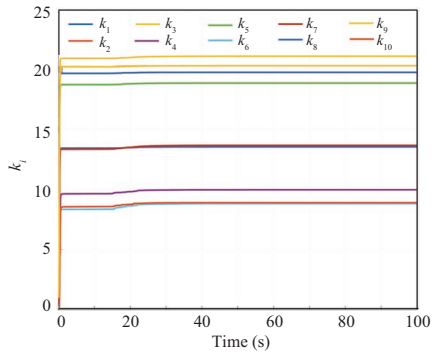


Fig. 7. Adaptive feedback gains $\{k_i\}$ of the structure observers $\{u_i(t)\}$ versus time t.

5. Conclusion

This paper addresses the intralayer structure reconstruction of an arbitrary unknown layer in general weighted output-coupling multilayer complex dynamical networks based on generalized synchronization principles. The proposed reconstruction method incorporates a cross-layer coupling modulator and a structural divergence term into the design of adaptive structure observers. By leveraging the simpler structural information from a known reference layer, the structure observers enable reconstructing the structure of the target layer and real-time monitoring the abrupt structure changes through co-processing generalized synchronization. A key feature of the proposed method is its ability to arbitrarily select the target and the reference layers from the output-coupling multilayer network, enhancing flexibility across diverse network configurations. Numerical simulations validate the effectiveness and efficiency of the proposed reconstruction method for intralayer structure reconstruction and monitoring. In subsequent studies, the interlayer coupling interactions can be extended into more general node-dependent forms, enabling arbitrary nodes across any layers to form independent coupling connections, which will capture more complex real-world scenarios. Practical engineering considerations, such as measurement noise, system uncertainties, heterogeneous node dynamics, are identified as promising directions for future research.

Acknowledgments

Project supported by the National Natural Science Foundation of China (Grant No. 62373197), the Natural Science Foundation of the Higher Education Institutions of Jiangsu Province, China (Grant No. 23KJB120010), the Industry–University–Research Cooperation Project of Jiangsu Province, China (Grant No. BY20251038), and the Cultivation and Incubation Project of the College of Automation, Nanjing University of Posts and Telecommunications.

References

[1] Pulvermüller F, Tomasello R, Henningsen-Schomers M R and Wennekers T 2021 *Nat. Rev. Neurosci.* **22** 488
[2] Shen Y, Wang J and Navlakha S 2021 *Neural Comput.* **33** 3179
[3] Lin X, Yu R, Yu J and Wen H 2022 *IEEE Trans. Ind. Electron.* **70** 11310
[4] Shao X G, Zhang J and Lu Y J 2024 *Chin. Phys. B* **33** 070203
[5] Hu H X, Wen G, Chen Y and Zheng W X 2024 *Automatica* **169** 111840
[6] Yang P, Fan R, Wang Y and Zhang Y 2024 *Chin. Phys. B* **33** 070206
[7] D'Souza R M, di Bernardo M and Liu Y Y 2023 *Nat. Rev. Phys.* **5** 250
[8] Liang X S 2021 *Chaos* **31** 093123
[9] Li X, Zhang H, Shen Y, Hao L and Shang W 2022 *IEEE Trans. Intell. Transp. Syst.* **24** 13330
[10] Lin J C, Fan R G, Wang Y Y and Du K 2023 *Chin. Phys. B* **32** 100502
[11] Muhtadi A, Pandit D, Nguyen N and Mitra J 2021 *IEEE Trans. Ind. Appl.* **57** 2223
[12] Isufi E, Gama F, Shuman D I and Segarra S 2024 *IEEE Trans. Signal Process.* **72** 4745
[13] Sun Y, Lei L, Guan D, Kuang G and Liu L 2022 *IEEE Trans. Geosci. Remote Sens.* **60** 1
[14] Li J, Sun Q, Peng H, Yang B, Wu J and Yu P S 2023 *IEEE Trans. Pattern Anal. Mach. Intell.* **45** 8063
[15] Fei J and Liu L 2021 *IEEE Trans. Ind. Electron.* **69** 8366
[16] Zheng Y, Zhang H T, Yue Z and Wang J 2024 *IEEE Trans. Neural Netw. Learn. Syst.* **35** 8063
[17] Massignan J A, London J B, Bessani M, Maciel C D, Fannucchi R Z and Miranda V 2021 *IEEE Trans. Smart Grid* **13** 526
[18] Li Y, He J, Chen C and Guan X 2023 *IEEE Trans. Autom. Control* **69** 3483
[19] Liu X, Shao Q and Chen D 2024 *IEEE Trans. Artif. Intell.* **5** 3445
[20] Karimi H S and Natarajan B 2021 *IEEE Trans. Smart Grid* **12** 5299
[21] Zhang Y, Yang C, Huang K, Jusup M, Wang Z and Li X 2020 *IEEE Trans. Emerg. Top. Comput. Intell.* **5** 920
[22] van Waarde H J, Tesi P and Camlibel M K 2019 *IEEE Trans. Autom. Control* **64** 4300
[23] Sharf M and Zelazo D 2023 *IEEE Trans. Control Netw. Syst.* **10** 1616
[24] Zhao J L, Zhang X J, Ding X, Zhang X and Zhang H F 2025 *IEEE Trans. Netw. Sci. Eng.* **12** 2333
[25] Zhang H F, Xu F, Bao Z K and Ma C 2018 *IEEE Trans. Circuits Syst. I: Reg. Pap.* **66** 1608
[26] Li X, Lin L, Liu Q, Kong Z and Ding L 2021 *IEEE Trans. Comput. Soc. Syst.* **10** 24
[27] Zhu S, Zhou J, Chen G and Lu J A 2019 *IEEE Trans. Cybern.* **51** 2224
[28] Xu Y, Zhou W, Zhang J, Sun W and Tong D 2017 *Nonlinear Dyn.* **88** 2969
[29] Veedu M S and Salapaka M V 2023 *Automatica* **156** 111182
[30] Zhang C, Chen H, Xu Q, Feng Y and Li R 2024 *Nonlinear Anal. Hybrid Syst.* **51** 101431
[31] Wang Y, Wu X, Feng H, Lu J and Lü J 2016 *Sci. China Technol. Sci.* **59** 1232
[32] Yan J, Zhou J and Wu Z 2019 *Physica A* **525** 256
[33] Chen X, Zhang J and Ma T 2016 *IEEE/CAA J. Autom. Sinica* **3** 295
[34] Chen H, Zhang C and Yang H 2025 *IEEE Trans. Neural Netw. Learn. Syst.* **36** 8063
[35] Zheng Y, Wu X, He G and Wang W 2021 *Chaos* **31** 043125
[36] Chen C, Zhou J, Qu F, Song C and Zhu S 2022 *Commun. Nonlinear Sci. Numer. Simul.* **115** 106779
[37] Fan Z and Wu X 2022 *Chaos* **32** 113128
[38] Ma C, Lin Q, Lin Y and Ma X 2021 *Knowl.-Based Syst.* **213** 106666
[39] Wu X, Fan Z, He J, Wang W and Lü J 2023 *IEEE Trans. Syst., Man, Cybern.: Syst.* **53** 7794
[40] Wang Y, Wu X, Lü J, Lu J A and D'Souza R M 2018 *IEEE Trans. Netw. Sci. Eng.* **7** 538
[41] Liu H, Li Y, Li Z, Lü J and Lu J A 2021 *IEEE Trans. Cybern.* **52** 6255
[42] Zheng Y, Wu X, Fan Z, Chen K and Lü J 2025 *IEEE Trans. Cybern.* **55** 3445
[43] Wang X, Lü J and Wu X 2018 *IEEE Trans. Syst., Man, Cybern.: Syst.* **50** 2588
[44] Li G, Li N, Liu S and Wu X 2019 *Chaos* **29** 053117
[45] Zhang C, Yang H, Zhou J and Zhou H 2024 *IEEE Trans. Autom. Sci. Eng.* **21** 4745
[46] Zhao X, Zhou J, Zhu S, Ma C and Lu J A 2019 *IEEE Trans. Circuits Syst. II: Express Briefs* **67** 290
[47] Bao H, Park J H and Cao J 2020 *IEEE Trans. Neural Netw. Learn. Syst.* **32** 3230
[48] Qiu Q and Su H 2022 *IEEE Trans. Netw. Sci. Eng.* **9** 1386
[49] Liu H, Shang Z, Ren Z, Li Y, Zeng Z and Lu J 2022 *Sci. China Technol. Sci.* **65** 1493
[50] Tao G 1997 *IEEE Trans. Autom. Control* **42** 698